

## Effect of Structural Symmetry on Gas Transport Properties of Polysulfones

C. L. Aitken, W. J. Koros, and D. R. Paul\*

Department of Chemical Engineering and Center for Polymer Research, The University of Texas at Austin, Austin, Texas 78712

Received February 10, 1992

**ABSTRACT:** The effects of structural symmetry of phenylene linkages and methyl group placement on the properties of polysulfones have been investigated. Polysulfones with unsymmetric structures have lower gas permeability and higher selectivity coefficients than their symmetric counterparts. The polysulfones with *m*-phenylene linkages or dimethyl substitutions to the bisphenol unit have lower glass transition temperatures, lower fractional free volumes, and higher sub- $T_g$  relaxation temperatures. The chains of the unsymmetric polymers are generally more efficiently packed and appear to have greater mobility constraints, stemming from both intramolecular and intermolecular origins, than their symmetric counterparts, all of which influence properties and especially permeation behavior.

### Introduction

Recent studies have revealed interesting effects of structural symmetry on the gas transport properties of a number of polymers including polyimides,<sup>1-4</sup> polyesters,<sup>5</sup> poly(phenolphthalein phthalates),<sup>6</sup> and poly(methyl methacrylate).<sup>7</sup> For the polymers with aromatic rings in their backbones, changing the connecting bond positions from para to meta appears to reduce their permeability to gases. Symmetrical placement of methyl groups on the backbone phenyl rings of polysulfones<sup>8</sup> and polycarbonates<sup>9</sup> increases gas permeability, while unsymmetrical addition leads to a decrease at least for polysulfone. Symmetry effects are of interest because they provide a means to improve the barrier or separation properties of membrane materials, and fundamental investigations of their influence should lead to further insights about how interchain packing and chain flexibility affect gas permeability.

The present work further explores some effects of structural symmetry on the gas transport properties of modified polysulfones and is part of a broader, detailed investigation of the relationships between structure and the gas transport properties of polysulfones and polycarbonates<sup>8-15</sup> prompted by their commercial importance as membrane materials. For more than a decade, the polysulfone based on Bisphenol A has been widely used to form commercial hollow fiber membranes for gas separations. More recently, tetrabromo-Bisphenol A polycarbonate-type materials have also been used for this purpose. The design of new materials to meet increased performance requirements for gas separation membranes demands a better understanding of the relationship between chemical structure, including the effect of symmetry, and gas transport properties. Gas permeation and sorption measurements are complemented by a variety of experimental techniques including X-ray diffraction, differential scanning calorimetry, dilatometry, thermogravimetric analysis, and dynamic mechanical analysis.

### Background

The literature contains several examples of polymers with aromatic backbones where the unsymmetrical isomers have a significantly lower  $T_g$  and specific volume relative to their symmetrical isomers.<sup>1-7</sup> Light and Seymour,<sup>5</sup> in their study of aromatic polyesters, observed that poly(ethylene isophthalate) (PEI) not only has a lower  $T_g$  than

poly(ethylene terephthalate) (PET) but also has an  $O_2$  permeability coefficient about half that for PET. In more recent studies of poly(phenolphthalein phthalates), Sheu and Chern found that the glass transition temperatures of the *m*-phenylene isomers are about 50 °C lower than those for the para form<sup>6</sup> and that the gas permeabilities of the isophthalate structure are much lower than that of the terephthalate structure. A review of other studies on spatial configuration effects for a variety of polymers suggests that a higher  $T_g$  for the para structure is general.<sup>6</sup>

Min and Paul compared gas transport properties of isotactic (i-PMMA), syndiotactic (s-PMMA), and atactic (a-PMMA) poly(methyl methacrylate).<sup>7</sup> The isotactic form has a higher density, a lower  $T_g$ , and a lower gas permeation coefficient than the syndiotactic material. It was suggested that the difference between the specific volumes and, hence, permeabilities of these isomeric forms is at least partially a result of the quite large difference in their glass transition temperatures. The isomers have relatively similar densities in the melt state; thus, i-PMMA will tend to be more dense in the glassy state simply because it has to be cooled further, at the high thermal contraction rate of the rubbery form, to reach its  $T_g$  than does s-PMMA. This effect alone should lead to a lower diffusivity. The gas solubility coefficients for i-PMMA are about one-third those for s-PMMA. This was attributed to smaller contributions from the Langmuir sorption capacity term of the dual sorption model for the former owing to the smaller unrelaxed volume in the glassy state relative to the equilibrium liquid state because of its lower  $T_g$ . The lower permeability for the isotactic form appears to arise from both lower solubility and diffusivity of gases, and both of these factors are a function of the packing density.

Several studies of polyimides<sup>1-4</sup> have revealed that relatively large increases in permselectivity are obtained when para linkages are replaced with meta linkages. For example, the meta-connected polyimide 6FDA-6FmDA, studied by Coleman and Koros,<sup>1</sup> has an  $O_2/N_2$  selectivity that is 50% higher than that of the para isomer 6FDA-6FpDA. The polyimide structures are shown in Table I. In this study, the location of the phenylene bond had a more dramatic effect on the transport properties than did the replacement of the isopropylidene group with the bulkier hexafluoroisopropylidene unit. It was proposed that these changes in permeability and permselectivity may arise from a restriction in the sub- $T_g$  motions of the unsymmetric polyimides.

\* Author to whom correspondence should be addressed.

Table I  
Structures for Polyimides Discussed in the Text

polyimide	structure
PMDA-ODA	
PMDA-BDAF	
6FDA-6FDA	

Stern et al.,<sup>2</sup> evaluated several other polyimide isomer pairs that also illustrate the effect of bond placement on transport properties. The permeability coefficients for the symmetric polyimide PMDA-4,4'-ODA are reported to be about twice that of the unsymmetric PMDA-3,3'-ODA polymer, while the permselectivity for the unsymmetric polymer is almost twice that of the symmetric material for several gas pairs. However, another unsymmetric polyimide, PMDA-3,3'-BDAF, appears to have only slightly enhanced permselectivity relative to that of PMDA-4,4'-BDAF. They suggest that the lower permeability and higher selectivity of the meta-linked polymers may be a result of hindered rotation about the meta-connected ether linkage. They refer to the work of Pavlova et al.,<sup>16</sup> in which a Monte Carlo simulation predicts that rotation about nonlinear phenylene bonds is forbidden for diamine moieties. In the PMDA-3,3'-ODA case, all of the flexible ether linkages have meta bonds, whereas in the PMDA-3,3'-BDAF polymer only half of the phenylene-ether connections are unsymmetric. Thus, these authors suggest that PMDA-3,3'-BDAF has more flexible oxygen linkages that lead to higher permeability.

Tanaka et al.,<sup>4</sup> in a study of polyimide isomers, suggested that the reason for the lower  $T_g$  of the meta isomers stems from their higher configurational entropy due to a larger degree of conformational freedom of the main chains than the para-linked polymers. Attempts have been made in the literature to correlate the glass transition temperature with a calculated measure of conformational entropy since this should be an indicator of molecule flexibility.<sup>17-20</sup> Sundararajan reports good success for symmetrically substituted polycarbonates, but the correlation does not hold as well for polycarbonates with unsymmetric connecting groups.<sup>17</sup> The  $T_g$  is lower for this type of unsymmetrical material than the correlation with the calculated partition function or conformational entropy would indicate.

In a study of poly(phenylene oxides), Tonelli concluded that the large  $T_g$  range caused by various ring substitutions cannot be explained by intramolecular barriers since these barriers are so small and similar for the materials he considered.<sup>18</sup> He also noted that the  $T_g$  of the unsymmetric poly(2-methyl-6-phenyl-1,4-phenylene oxide) is substantially lower than that for the symmetric poly(2,6-dimethyl-1,4-phenylene oxide) (PPO), which does not conform to the trends he expected from intermolecular interactions, based mainly on the bulkiness of pendant groups.

Symmetry appears to have the opposite effect on  $T_g$  for carbon chain polymers. The symmetric vinylidene polymers have lower glass transition temperatures than do the corresponding unsymmetrical vinyl polymers.<sup>21-23</sup> In comparison of the permeability characteristics of these materials, crystallinity effects have to be taken into account, which varies according to tacticity for vinyl polymers. For structural comparisons of this type, it is most convenient to refer to the behavior of purely amorphous materials. On this basis, Mohr and Paul<sup>21</sup> found a tendency for the symmetrical vinylidene polymers to have both lower fractional free volume and lower permeability coefficients than the corresponding unsymmetric vinyl polymers (e.g., pendant  $\text{CH}_3$  or  $\text{Cl}$  groups), which stands in contrast to the effects of symmetry noted above for polymers with aromatic backbones. Poly(vinylidene fluoride) (PVDF) is an exception to this trend since it has a higher permeability and slightly higher free volume than poly(vinyl fluoride) (PVF); however, the  $T_g$  for the symmetric polymer PVDF is still much lower than that for the unsymmetric polymer PVF. Gibbs and Di Marzio proposed that the low  $T_g$  for PVDF may be due to a relatively low energy barrier to rotation between stable conformations.<sup>24</sup>

## Experimental Section

All of the polysulfones described here were synthesized in our laboratories via nucleophilic condensation reactions. The bisphenol monomers were obtained from Kennedy and Klim with the exception of tetramethyl-Bisphenol M (Bisxylenol M), which was custom synthesized by Polysciences, Inc. The modified bisphenol monomers were reacted with 4,4'-difluorophenyl sulfone, from Aldrich Chemical Co., Inc., to form polysulfones according to the synthesis procedure developed by Mohanty<sup>25,26</sup> and modified by McHattie.<sup>13,27</sup> Monomers were purified by sublimation and reacted in *N*-methylpyrrolidinone (NMP) and toluene containing anhydrous  $\text{K}_2\text{CO}_3$ . The reaction temperature was increased to 165 °C over 6 h as water was removed from the mixture. After 3 h at 165 °C, the polymerization was continued at 175 °C for approximately 8 more h. After synthesis, special attention was given to solvent removal from the polymer product. The polymers were precipitated in ethanol several times and then washed by Soxhlet extraction in water and ethanol for 3 days each. In addition, the polymers were dried at 60 °C under vacuum for 1 week. Intrinsic viscosity measurements at 25 °C are used as a relative indication of molecular weight.

Dense films of 1–3 mil were prepared by solution casting from methylene chloride onto glass plates. The films were dried at 60 °C for 1 week, and then the temperature was increased by 50 °C/day to approximately 20 °C >  $T_g$  and held there for 1 day.

To standardize thermal history, all films were rapidly quenched from above the  $T_g$  to room temperature with the exception of TMPSF-M, which degraded or cross-linked at elevated temperatures and, thus, was not exposed to temperatures greater than 60 °C. All polymer solutions were passed through 2- $\mu$ m Teflon filters prior to casting to remove particulate contamination.

Thermogravimetric analysis (TGA) and differential scanning calorimetry (DSC) were used to ensure solvent-free films. Residual solvent can be detected using TGA by observing any weight loss at temperatures below the degradation temperature. The TGA was operated at a heating rate of 20 °C/min up to the polymer degradation temperature ( $T_d$ ). A Perkin-Elmer differential scanning calorimeter (DSC) was used to measure the glass transition temperature of the polymers at a heating rate of 20 °C/min. The  $T_g$  was calculated from the second trace using the midpoint method. Solvent contamination also can be detected by observing any difference between the  $T_g$ s measured in the first and second heats. All of the polymers were found to be amorphous with no crystalline melting point.

An Imass Autovibron dynamic mechanical viscoelastomer or Rheovibron was used to measure the mechanical spectra of the polymer films at an operating frequency of 110 Hz. The temperature range was -150 to 200 °C with a heating rate of 1 °C/min.

Wide-angle X-ray diffraction measurements (WAXD) were taken at a wavelength of 1.54 Å on a Philips APD 3520 X-ray diffractometer. For these amorphous materials there is no long-range order; thus, a broad peak characteristic of the most probable distance between chains was observed. The  $d$  spacing calculated with Bragg's equation,  $n\lambda = 2d \sin \theta$ , is an approximate average distance between the axes of neighboring chains in the polymer matrix.

The densities of the polymers were determined by a density gradient column based on aqueous solutions of calcium nitrate at 30 °C. The measured densities were then used to calculate fractional free volumes (FFV) as described elsewhere.<sup>8,28,29</sup>

For several polymers, pressure-volume-temperature (PVT) measurements were made using a commercial dilatometer that has been described in detail elsewhere.<sup>30,31</sup> Thermal expansion isobars were obtained over a temperature range of 30–300 °C with a heating rate of 1.5 °C/min. Experiments were conducted at pressures of 10, 20, 50, and 100 MPa. The minimum pressure for accurate isobaric measurements with this PVT equipment is 10 MPa.

Pure gas permeability coefficients were measured for 3,4'-PSF, PSF-M, PSF-P, TMPSF-M, and TMPSF-P. The data for PSF and TMPSF from McHattie<sup>8</sup> are included for comparison. Permeability coefficients for six chromatographic grade gases were determined at 35 °C for pressures up to 20 atm using permeation cells previously described.<sup>32</sup> Due to the brittleness of 3,4'-PSF and PSF-M, only low-pressure permeation measurements were possible. The gases were tested in the following order: He, H<sub>2</sub>, O<sub>2</sub>, N<sub>2</sub>, CH<sub>4</sub>, and CO<sub>2</sub>. Conditioning effects were noted, when possible, by observing any change in the permeability of a gas at 1 atm after exposure to 20 atm of the same gas. Pure gas sorption isotherms were measured with pressure decay cells that have been described extensively in previous papers.<sup>32</sup> The sorption levels were measured from 1 to 20 atm with nitrogen, methane, and carbon dioxide.

### Effect of Symmetric and Unsymmetric Phenylene Linkages

The pure gas permeability coefficients for PSF-P, TMPSF-P, and TMPSF-M are shown as a function of pressure in Figures 1–3. The permeability coefficients remain constant or decrease with pressure in all cases. No plasticization and only minimal conditioning effects were observed at these pressures.

The permeability and selectivity coefficients for each polymer structure are shown in Table II. Consistently, replacement of a *p*-phenylene bond with a meta linkage results in a suppression of the permeability and an increase in the selectivity. The permeability coefficients for 3,4'-PSF are approximately 3–4 times lower than those for

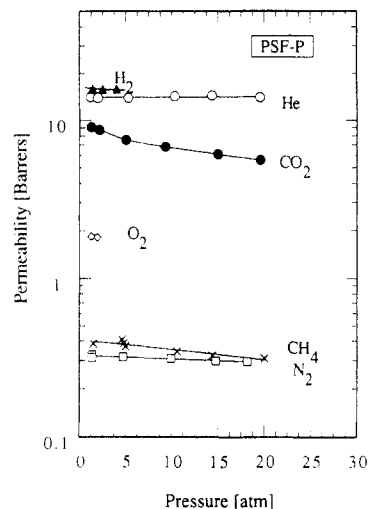


Figure 1. Pressure dependence of He, H<sub>2</sub>, O<sub>2</sub>, N<sub>2</sub>, CH<sub>4</sub>, and CO<sub>2</sub> permeability coefficients for PSF-P at 35 °C.

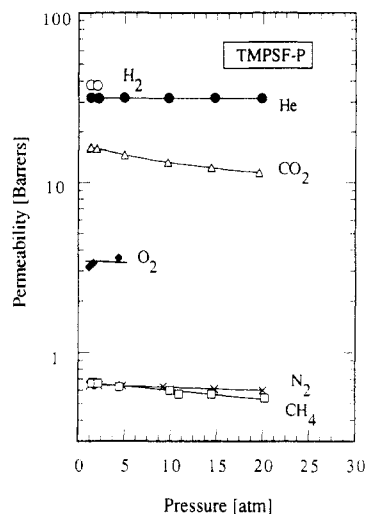


Figure 2. Pressure dependence of He, H<sub>2</sub>, O<sub>2</sub>, N<sub>2</sub>, CH<sub>4</sub>, and CO<sub>2</sub> permeability coefficients for TMPSF-P at 35 °C.

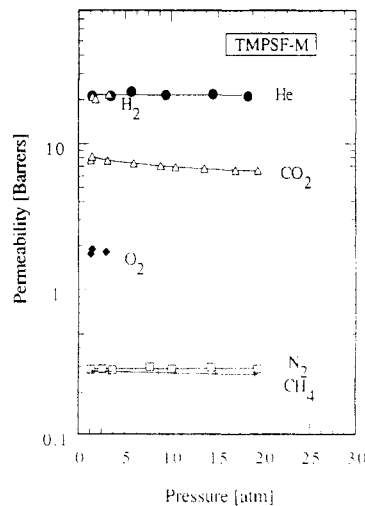
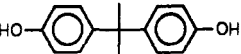
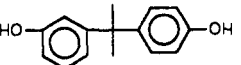

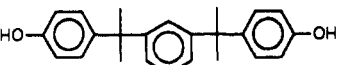
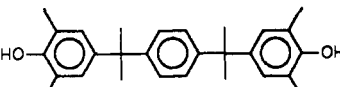
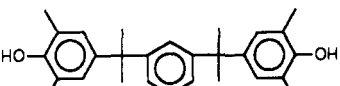
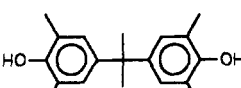


Figure 3. Pressure dependence of He, H<sub>2</sub>, O<sub>2</sub>, N<sub>2</sub>, CH<sub>4</sub>, and CO<sub>2</sub> permeability coefficients for TMPSF-M at 35 °C.

PSF. However, the permeability coefficients for the small gases He and H<sub>2</sub> only decrease by about 30% and, thus, there is an increase in the selectivity for the He/CH<sub>4</sub> separation. A comparison of PSF-P and PSF-M shows the same trend. Again, the meta isomer is the less permeable but more selective material. The He/CH<sub>4</sub> separation factor is greater than 100.

Table II  
Permeability and Selectivity Coefficients for Para and Meta Linked Polysulfones

polymer	bisphenol monomer	$P_{\text{CO}_2}$ , <sup>a</sup> barrer <sup>b</sup>	$\alpha^*_{\text{CO}_2/\text{CH}_4}$ <sup>a</sup>	$P_{\text{O}_2}$ , <sup>c</sup> barrer <sup>b</sup>	$\alpha^*_{\text{O}_2/\text{N}_2}$ <sup>c</sup>	$P_{\text{H}_2}$ , <sup>a</sup> barrer <sup>b</sup>	$\alpha^*_{\text{H}_2/\text{CH}_4}$ <sup>a</sup>	$\alpha^*_{\text{H}_2/\text{H}_2}$ <sup>c</sup>
PSF		5.6	22	1.4	5.6	13	49	0.93
3,4'-PSF		1.5 <sup>c</sup>	29 <sup>c</sup>	0.39	5.9	9.3 <sup>c</sup>	180 <sup>c</sup>	1.16
PSF-P		6.8	20	1.8	5.6	14	41	0.84
PSF-M		2.8 <sup>c</sup>	25 <sup>c</sup>	0.69	6.3	11.7 <sup>c</sup>	104 <sup>c</sup>	1.1
TMPSF-P		13.2	22	3.2	5.6	32	53.3	0.9
TMPSF-M		7.0	25	1.8	6.4	21	76.5	1.04
TMPSF		21	22	5.6	5.3	41	45	1.3

<sup>a</sup> Data at 10 atm. <sup>b</sup> Barrer =  $10^{-10}[\text{cm cm}^3(\text{STP})]/(\text{cm}^2 \text{ s cmHg})$ . <sup>c</sup> Data at 1 atm.

It has been shown in previous studies<sup>8-10,14</sup> that the symmetrical addition of four methyl groups onto the bisphenol rings of polycarbonates and polysulfones results in an increase in permeability without a significant loss in selectivity. Thus, TMPSF-M combines the attractive permeability characteristics of the tetramethyl addition with the desirable selectivity of a meta linkage. The unsymmetric TMPSF-M exhibits lower permeability but higher selectivity than the symmetric TMPSF-P; however, the differences between these isomers are not quite as dramatic as for the other isomer pairs, no doubt because the effect is diluted by the other para linkages in the long repeat unit. Note that TMPSF-M is simultaneously slightly more permeable and selective than Bisphenol A polysulfone.

Lengthening the Bisphenol A monomer unit of polysulfones by the additional phenylisopropylidene group in PSF-P results in slightly higher permeability but lower selectivity coefficients than PSF. In contrast, TMPSF-P has much lower permeability but higher selectivity coefficients than TMPSF because of the dilution effect mentioned earlier.

To better understand the transport through these materials, it is useful to separate the permeability coefficient into its kinetic and thermodynamic components.<sup>2,9,33</sup> The  $\text{N}_2$ ,  $\text{CH}_4$ , and  $\text{CO}_2$  sorption isotherms for the polymers in this study are shown in Figure 4-6. The solubility coefficients listed in Tables III and IV were calculated from the secant slope of these isotherms at 10 atm. The diffusion coefficients can be calculated from

$$P = \bar{D}\bar{S} \quad (1)$$

The oxygen diffusion coefficients listed in Table IV were computed from transient permeation time lag data allowing the  $\text{O}_2$  solubility coefficients to be calculated from eq 1. For each gas, the unsymmetric polymers have lower solubility and diffusion coefficients than their symmetric isomer. Both solubility and diffusivity appear to contribute to the decrease in permeability for the meta-linked polysulfones.

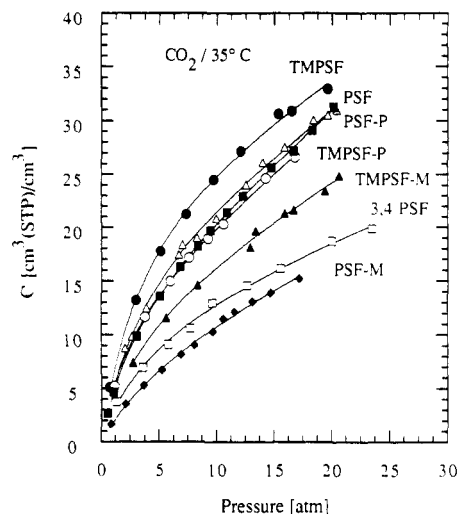


Figure 4. Sorption isotherms for  $\text{CO}_2$  at 35 °C.

The permselectivity is factored into diffusivity and solubility selectivity terms in Tables III and IV. These data show that replacing para linkages with meta linkages decreases the solubility factor but increases the diffusive term. The overall increase in permselectivity is the result of the larger increase in the diffusivity term.

The sorption and transport characteristics of these polymers are well described by the dual mode transport model:

$$C = k_D p + \frac{C_H' b p}{1 + b p} \quad (2)$$

$$P = k_D D_D + \frac{D_H C_H' b}{1 + b p_2} \quad (3)$$

The sorption and transport parameters, obtained by fitting of the data to eq 2, are listed in Table V. The Langmuir capacity term  $C_H'$  is consistently lower for the meta-linked than for the para-linked polysulfones. In general, for polymers with similar thermal expansion coefficients, the

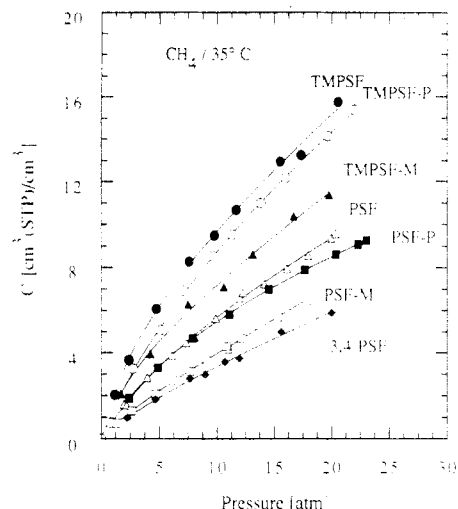


Figure 5. Sorption isotherms for CH<sub>4</sub> at 35 °C.

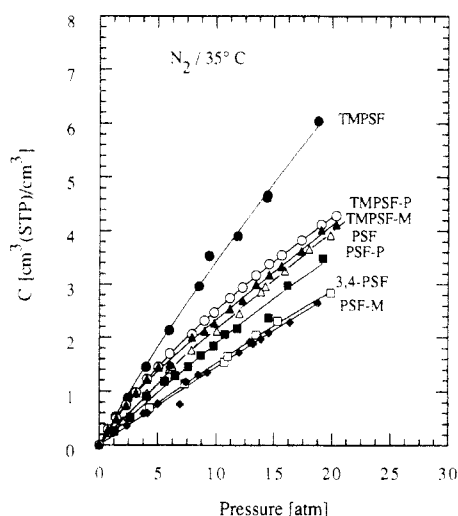


Figure 6. Sorption isotherms for N<sub>2</sub> at 35 °C.

Langmuir capacity term increases with  $T_g$ ,<sup>36,37</sup> and these polymers follow that trend. The affinity parameter  $b$  is slightly larger for the unsymmetric polymers. The Henry's law coefficient,  $k_D$ , does not consistently decrease with the meta substitution. To obtain the Henry's law and Langmuir mode diffusion coefficients,  $D_D$  and  $D_H$ , the permeability data were plotted vs  $1/(1 + bp_2)$ , where  $p_2$  is the upstream driving pressure, as suggested by eq 3. The results calculated from the slopes and intercepts are listed in Table V.

Both the X-ray  $d$  spacing and the fractional free volume, FFV, have been used to characterize the openness of polymer structure. The fractional free volume used here was calculated from

$$\text{FFV} = (V - V_o)/V \quad (4)$$

where  $V$  is the specific volume computed from the measured density and  $V_o$  is the occupied chain volume obtained using the Bondi group contribution method described elsewhere.<sup>8,28,29,38</sup> Several authors have demonstrated good correlations between the gas permeability of various polymers and FFV.<sup>8,14,38</sup> Table VI shows that the  $d$  spacings of PSF and 3,4'-PSF are about the same, while the  $d$  spacings of PSF-M and TMPSF-M are lower than those of their para isomers. The unsymmetric isomers are consistently more dense than their symmetric counterparts. Since the chemical compositions of the isomers are the same, the higher density of the unsymmetric structures directly reflects the lower free volume available

relative to the symmetric molecules. Figure 7 shows a rather good correlation of oxygen permeability for a number of polysulfones with the reciprocal of their fractional free volume. Likewise, Figure 8 suggests there is a relationship between the solubility coefficient for CO<sub>2</sub> and the fractional free volume, although the scatter is somewhat greater than seen in Figure 7. The current materials are shown by open symbols identified by their acronym. The points not identified are for other polysulfones described elsewhere.<sup>10-13,39</sup>

It may be noted in Figure 7 that the permeability coefficients for the unsymmetric polymers often tend to be slightly lower than that predicted by their fractional free volumes. Since the permeability measurements are believed to be quite accurate, these deviations may reflect either a somewhat different relationship with free volume for the unsymmetrically linked materials or errors in the evaluation of FFV. The polymer that lies furthest off the correlation line is 3,4'-PSF. A density of 1.259 g/cm<sup>3</sup> would be required to make the permeability of this polymer fall on the correlation line with FFV, which is an unreasonable value since the density of this material was experimentally determined to be  $1.250 \pm 0.0005$  g/cm<sup>3</sup>. Another possible source of error is in the estimation of the occupied volume,  $V_o$ , from group contribution terms. Van Krevelen<sup>28</sup> lists the same van der Waals volumes for phenylene rings with meta linkages as for those with para linkages. It is, however, possible that the occupied volumes of the two ring types are different. For example, if the van der Waals volume for the unsymmetric ring were 44.95 cm<sup>3</sup>/mol rather than 43.32 cm<sup>3</sup>/mol as reported, then the O<sub>2</sub> permeation coefficient for 3,4'-PSF would fall right on the correlation line in Figure 7. The free volumes for the other meta-linked polymers, PSF-M and TMPSF-M, would also decrease but are less affected by the value used for the unsymmetric phenyl ring volume since this ring is a smaller fraction of the repeat unit for these polymers. Therefore, if the occupied volume for the meta-linked phenyl is slightly higher than for the para-linked phenyl, the low permeability observed for the unsymmetric polymers would be well explained by their lower fractional free volume. There is still the possibility, however, that the correlation of permeability with fractional free volume follows a slightly different relationship for these materials.

In trying to rationalize the unexpected observation that meta-connected polymers have higher densities than their para counterparts, it may be tempting to seek an understanding based on the peculiarities of how long-chain molecules pack (i.e., chain conformational considerations). A brief survey of the packing behavior of small molecules in both the liquid and crystalline states provides some interesting insight. Table VII compares the densities of meta and para isomers of disubstituted benzene compounds obtained from chemical handbooks.<sup>40,41</sup> In the liquid state the meta isomer is frequently slightly more dense (<1%) than the para isomer. Consequently, the comparable effects seen in Table VI for polysulfones are not attributable solely to their long-chain character. On the other hand, for low molecular weight compounds in the crystalline state, the para isomer seems generally to be much more dense (>2%) than the corresponding meta isomer. Intuition suggests that when motion is suppressed and the molecules are ordered, the symmetrical isomer should achieve a higher density. This observation could also be rationalized, at least in part, by a smaller occupied volume of the para ring than of the meta ring as suggested earlier. The free volume in crystals is much lower than in the liquid (or glassy) state and, thus, small differences in occupied volume may become more apparent in crystals.

**Table III**  
**Solubility and Mobility Components of CO<sub>2</sub>/CH<sub>4</sub> Separation Factors<sup>a</sup>**

polymer	$P_{CO_2} \times 10^{10}$ , [cm cm <sup>3</sup> (STP)]/(cm <sup>2</sup> s cmHg)	$\alpha^*_{CO_2/CH_4}$	$\bar{S}_{CO_2}$ , cm <sup>3</sup> (STP)/(cm <sup>3</sup> atm)	$\bar{S}_{CO_2}/\bar{S}_{CH_4}$	$\bar{D}_{CO_2} \times 10^8$ , cm <sup>2</sup> /s	$\bar{D}_{CO_2}/\bar{D}_{CH_4}$
PSF	5.6	22	2.1	3.7	2.0	5.9
3,4'-PSF	1.5	29	1.3	3.6	0.9	7.7
PSF-P	6.8	20	2.1	3.9	3.2	5.3
PSF-M	2.8	25	1.1	2.6	2.7	9.5
TMPSF-P	13	22	2.0	2.2	5.0	9.9
TMPSF-M	7.0	25	1.6	2.1	4.5	11.0
TMPSF	21	22	2.5	2.7	6.4	8.1

<sup>a</sup> Data at 10 atm and 35 °C.

**Table IV**  
**Solubility and Mobility Components of O<sub>2</sub>/N<sub>2</sub> Separation Factors<sup>a</sup>**

polymer	$P_{O_2} \times 10^{10}$ , [cm cm <sup>3</sup> (STP)]/(cm <sup>2</sup> s cmHg)	$\alpha^*_{O_2/N_2}$	$\bar{S}_{O_2}$ , cm <sup>3</sup> (STP)/(cm <sup>3</sup> atm)	$\bar{S}_{O_2}/\bar{S}_{N_2}$	$\bar{D}_{O_2} \times 10^8$ , cm <sup>2</sup> /s	$\bar{D}_{O_2}/\bar{D}_{N_2}$
PSF	1.4	5.6	0.24	1.6	4.4	3.6
3,4'-PSF	0.39	5.9	0.17	1.5	1.7	4.0
PSF-P	1.8	5.6	0.43	2.4	3.2	2.4
PSF-M	0.69	6.3	0.23	1.6	2.3	3.9
TMPSF-P	3.2	5.6	0.38	1.5	6.0	3.5
TMPSF-M	1.8	6.4	0.33	1.4	4.1	4.5
TMPSF	5.6	5.3	0.53	1.4	8.0	3.8

<sup>a</sup> Data at 2 atm and 35 °C.

**Table V**  
**Dual Mode Sorption and Diffusion Coefficients**

polymer	gas	$k_D$ , cm <sup>3</sup> (STP)/(cm <sup>3</sup> atm)	$C_H'$ , cm <sup>3</sup> (STP)/cm <sup>3</sup>	$b$ , atm <sup>-1</sup>	$D_D \times 10^8$ , cm <sup>2</sup> /s	$D_H \times 10^8$ , cm <sup>2</sup> /s
PSF	N <sub>2</sub>	0.166	0.957	0.104	1.06	0.15
	CH <sub>4</sub>	0.257	6.58	0.0901	0.60	0.13
	CO <sub>2</sub>	0.728	19.6	0.260	4.64	0.58
3,4'-PSF	CH <sub>4</sub>	0.238	1.50	0.179	<i>a</i>	<i>a</i>
	CO <sub>2</sub>	0.407	12.70	0.219	<i>a</i>	<i>a</i>
PSF-P	N <sub>2</sub>	0.225	3.74	0.0461	1.13	0.44
	CH <sub>4</sub>	0.179	7.36	0.101	3.6	0.23
	CO <sub>2</sub>	0.905	14.95	0.303	5.6	1.28
PSF-M	N <sub>2</sub>	0.206	1.06	0.045	<i>a</i>	<i>a</i>
	CH <sub>4</sub>	0.311	1.19	0.247	<i>a</i>	<i>a</i>
	CO <sub>2</sub>	0.500	9.40	0.157	<i>a</i>	<i>a</i>
TMPSF-P	N <sub>2</sub>	0.131	2.57	0.088	4.24	0.56
	CH <sub>4</sub>	0.395	9.86	0.094	1.19	0.25
	CO <sub>2</sub>	0.860	14.26	0.375	13.09	1.44
TMPSF-M	CH <sub>4</sub>	0.379	4.76	0.249	0.69	0.02
	CO <sub>2</sub>	0.639	13.62	0.258	2.25	0.36
TMPSF	N <sub>2</sub>	0.225	3.74	0.0461	2.54	1.57
	CH <sub>4</sub>	0.460	7.26	0.233	1.22	0.16
	CO <sub>2</sub>	0.597	26.0	0.261	22.00	1.57

<sup>a</sup> Permeation data not taken as a function of pressure.

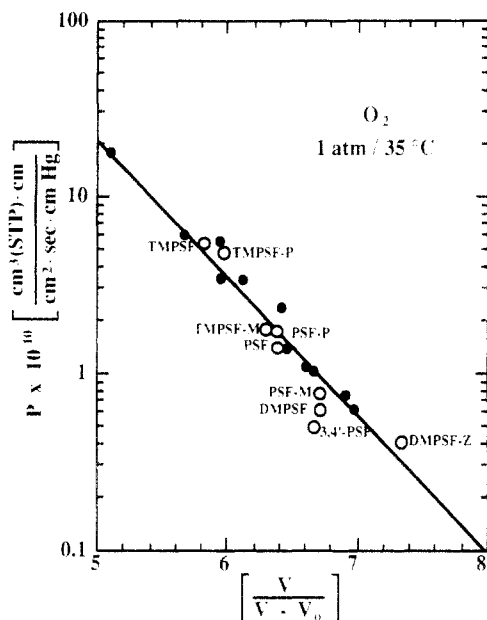
**Table VI**  
**Properties of Meta- and Para-Linked Polysulfones**

polymer	$T_g$ , °C	$T_\beta$ , °C	$T_{\gamma 1}$ , °C	$T_{\gamma 2}$ , °C	$\rho$ , g/cm <sup>3</sup>	FFV, $(V - V_0)/V$	$d$ spacing, Å	$[\eta]$ , <sup>a</sup> dL/g
PSF	186	85		-80	1.240	0.156	4.9	0.4
3,4'-PSF	156		?	-40	1.250	0.149	4.9	0.3
PSF-P	191			-85	1.191	0.156	4.9	1.3
PSF-M	140		40	-75	1.201	0.151	4.7	0.4
TMPSF-P	214		-10	-85	1.127	0.168	5.2	0.4
TMPSF-M	175		?	-90	1.141	0.158	5.1	0.3
TMPSF	230		-10	-92	1.151	0.171	5.3	1.1

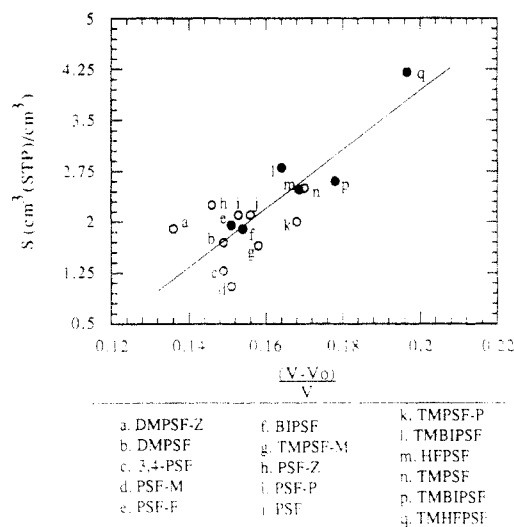
<sup>a</sup> In chloroform at 25 °C.

To examine the relationship between glass transition temperature and specific volume, the thermal expansion behavior of the polysulfone isomers was investigated via PVT measurements at 10 MPa as shown in Figure 9. Extrapolation to 0 MPa for PSF and PSF-P showed that the difference in thermal expansion coefficients at 0 and 10 MPa is not very significant; thus, it has been assumed that any error due to differences in compressibility among the polymers is small in Figure 9. In the melt state, the

specific volume of each unsymmetrical isomer is similar but slightly smaller than that of the corresponding symmetrical isomer. The difference in specific volume between the symmetrical and unsymmetrical isomers grows upon cooling because of the lower  $T_g$  of the latter. Interestingly, the thermal expansion coefficients of the two unsymmetrical isomers below  $T_g$  are similar but lower than that of the symmetrical isomers. Because of the latter, the differences in specific volumes at 35 °C between the



**Figure 7.** Correlation of the O<sub>2</sub> permeability coefficient with inverse fractional free volume calculated using the Bondi method. Open dots represent polysulfones reported here, while solid points are for polysulfones described elsewhere.<sup>8-12</sup>



**Figure 8.** Correlation of the CO<sub>2</sub> solubility coefficient at 35 °C with fractional free volume calculated using the Bondi method. Open dots represent polysulfones reported here, while solid points are for polysulfones described elsewhere.<sup>8-12</sup>

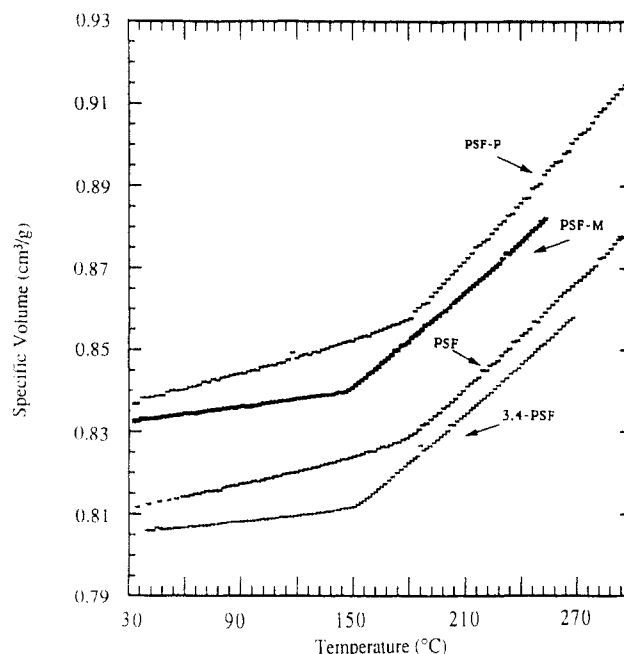
symmetric and unsymmetric isomers that can be attributed to the differences in  $T_g$  of the two are somewhat diminished.

The glass transition temperatures, listed in Table VI, for the para-linked polysulfones are significantly higher than those of the meta isomers. The  $T_g$  for PSF is 31 °C higher than that for 3,4'-PSF, the  $T_g$  of PSF-P is 51 °C higher than that for PSF-M, and the  $T_g$  of TMPSF-P is 39 °C higher than that for TMPSF-M. Lengthening of the Bisphenol A monomer causes PSF-P to have a  $T_g$  that is 5 °C higher than that for PSF. This suggests that the extra *p*-phenyleneisopropylidene unit increases the rigidity of the chain as the effect of the flexible ether linkages is diluted somewhat. Tetramethyl substitution on the PSF-P chain causes an increase in the glass transition temperature of 23 °C, which is less than the 44 °C difference between PSF and TMPSF. Comparing TMPSF and TMPSF-P reveals that the additional phenylisopropylidene group in the bisphenol monomer allows for more long-chain flexibility by diluting out the rigidity imparted by the tetramethyl substitution.

**Table VII**  
Comparison of the Density of Meta and Para Isomers of Low Molecular Weight Compounds in the Liquid and Crystalline States

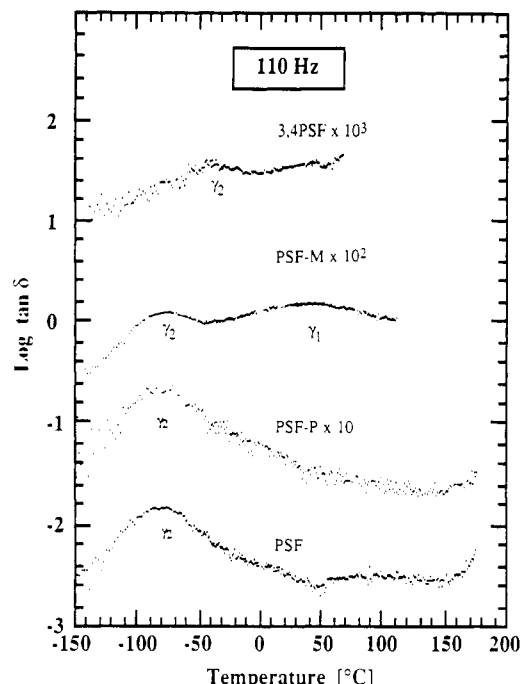
state	compound	$[(\rho_{\text{meta}} - \rho_{\text{para}})/\rho_{\text{para}}] \times 100^a$	temp. <sup>b</sup> °C
liquid	dimethylbenzene	0.10	20
liquid	methylethylbenzene	0.38	20
liquid	diethylbenzene	0.22	20
liquid	methylpropylbenzene	0.30	20
liquid	methylisopropylbenzene	0.58	20
liquid	diisopropylbenzene	-0.11	20
liquid	chlorotoluene	0.19	20
liquid	methylanisole	0.08	25
crystal	dihydroxybenzene	-4.2	15
crystal	dinitrobenzene	-3.1	20
crystal	chlorophenol	-2.9	20
crystal	bis(bromomethyl)benzene	-2.6	0

<sup>a</sup> Data from refs 42 and 43. <sup>b</sup> The densities of the meta and para isomers are compared at the same temperature in most cases; however, in a few instances the data are at temperatures that differ but by no more than 5 °C.

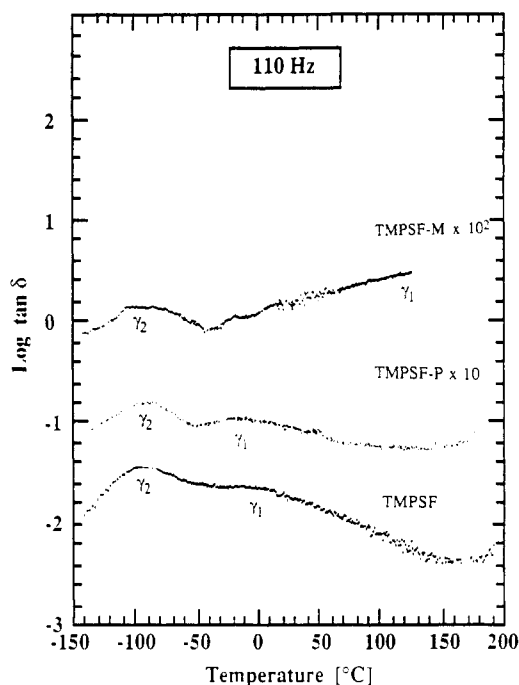


**Figure 9.** Thermal expansion behavior at 10 MPa for two sets of polysulfone isomers.

The sub- $T_g$  relaxations of these polymers have been discussed in a previous paper.<sup>42</sup> For convenience, the  $\tan \delta$  curves of the polysulfones of interest here are compared in Figure 10 and 11. While the sub- $T_g$  spectra of PSF and PSF-P are virtually identical, there is a clear splitting of the  $\tan \delta$  curve into two  $\gamma$  peaks for PSF-M. We have proposed previously that the  $\gamma_1$  peak has its origin in motions of the bisphenol unit, while the  $\gamma_2$  peak reflects motions characteristic of the diphenyl sulfone unit. Compared to PSF, polysulfone P has an additional *p*-phenylisopropylidene group in the recurring bisphenol monomer. Since these phenyls are similar to the phenyls in Bisphenol A polysulfone, it is not surprising that the sub- $T_g$  relaxations are similar. However, there is a difference in the relaxation spectra when the phenylene group is added in the meta position (PSF-M), viz., the latter exhibits separate  $\gamma_1$  and  $\gamma_2$  peaks. The  $T_{\gamma_1}$  for PSF-M is 115 °C higher than  $T_{\gamma_2}$  and is quite broad, perhaps reflecting the hindered mobility about the asymmetric meta linkage compared to that of the para linkage. It is anticipated that 3,4'-PSF has a similar high-temperature  $\gamma_1$  peak resulting from the meta linkage; however, due to



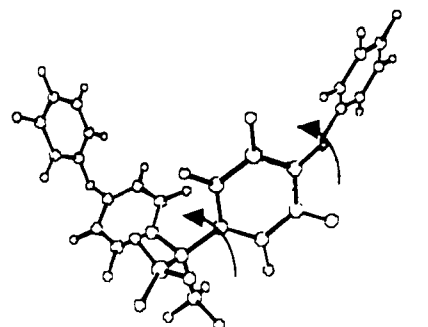
**Figure 10.** Tan  $\delta$  at 110 Hz as a function of temperature showing the sub- $T_g$   $\gamma$  peaks for polysulfone isomers. Assignments are described in the text.



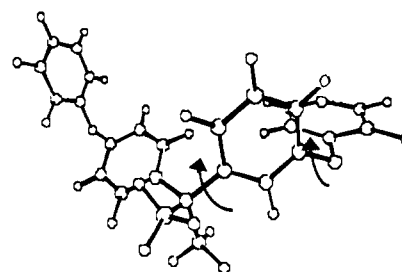
**Figure 11.** Tan  $\delta$  at 110 Hz as a function of temperature showing the sub- $T_g$   $\gamma$  peaks for tetramethyl polysulfone isomers. Assignments are described in the text.

the brittleness of this polymer, it could not be tested at temperatures greater than 80 °C.

As previously discussed, low-temperature peaks in the dynamic mechanical spectra of aromatic thermoplastics like polycarbonates and polysulfones have been associated with phenyl ring rotations or  $\pi$  flips. Space-filling molecular models illustrate the more hindered nature of an isolated 1,3-phenylene diol vs that of a 1,4-phenylenediol. It is apparent from these models that while an isolated para-linked phenyl ring can rotate rather freely, the meta-linked ring cannot complete a flip without moving the attached atoms. The cooperation of connected atoms is necessary for the *m*-phenyl ring rotation to occur. For a larger molecule, like the Bisphenol A polysulfone segment



Para-linked bisphenol A segment



Meta-linked bisphenol A segment

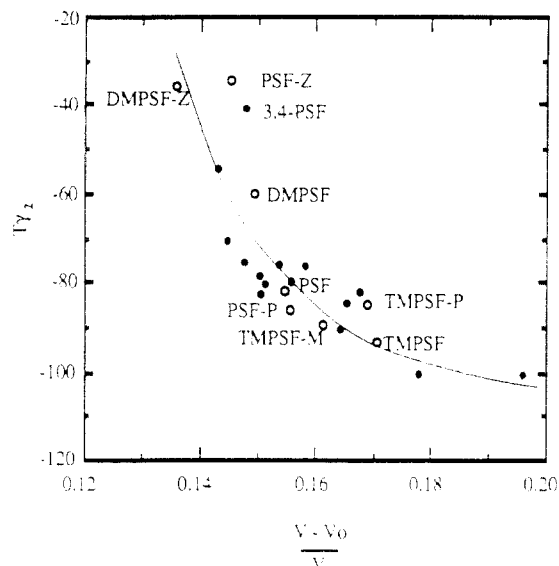
**Figure 12.** Perspective ball and stick drawing to illustrate the relative freedom for complete rotation for the para-linked phenyl vs that for the meta-linked phenyl in a Bisphenol A polysulfone segment.

illustrated in Figure 12, the *m*-phenylene rotation would also be blocked by adjacent groups and, thus, will require the concerted motion of attached units like the phenyl ring shown behind the meta-linked ring.

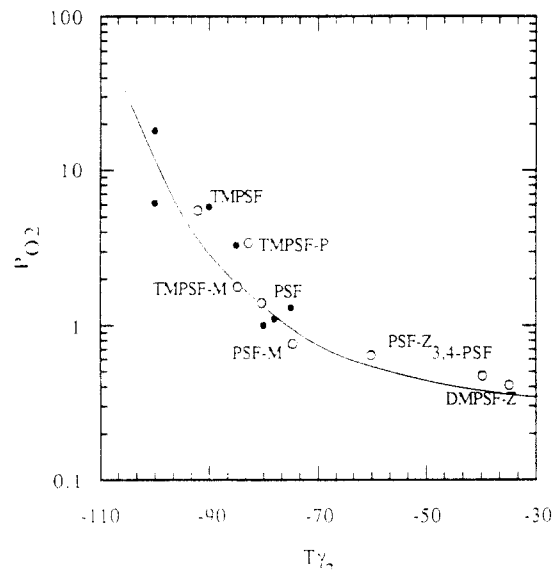
As in other cases of methyl ring substitution, TMPSF-P shows two  $\gamma$  peaks.<sup>8,12,42</sup> Additionally,  $T_{\gamma_2}$  is higher for TMPSF-P than for TMPSF. This implies that the lengthened bisphenol unit increases the ability of the chains to pack efficiently because of the increased number of available conformations and by dilution of the disruptions caused by the pendant methyl groups. The meta isomer, TMPSF-M, also has two sub- $T_g$  relaxations, with a much broader  $\gamma_1$  peak, like that of PSF-M. Dynamic mechanical data were not obtained for TMPSF-M above 150 °C due to brittleness of the film; hence, the temperature of the peak maximum,  $T_{\gamma_1}$ , is not listed in Table VI.

As discussed previously,<sup>10,42</sup> there is some intermolecular influence on the temperature at which the sub- $T_g$  relaxations occur. As proposed above, the  $\gamma_2$  relaxation stems from the diphenyl sulfone unit, which is the same for all of the polysulfones; hence, this peak should be a good indicator of intermolecular effects. For a broad range of polysulfones, Figure 13 shows how the temperature at which this peak is maximum depends on intermolecular chain packing or free volume. Polymers with low free volumes such as 3,4'-PSF have high  $T_{\gamma_2}$ . This indicates that as FFV decreases, intermolecular barriers to small-scale motions are increased and the relaxation occurs at a higher temperature. Figure 14 shows there is also a relationship between the  $O_2$  permeation coefficient and the  $T_{\gamma_2}$  for this series of polysulfones. It is quite likely that the motions associated with the  $\gamma_2$  peak do not regulate permeability, as the results in Figure 14 might suggest, but rather that both  $T_{\gamma_2}$  and permeability are influenced by free volume. Although there does seem to be an





**Figure 13.** Relationship between the sub- $T_g$  relaxation temperature  $T_{\gamma 2}$  and fractional free volume for various polysulfones. Open dots represent polysulfones reported here, while solid points are for polysulfones described elsewhere.<sup>8-12</sup>

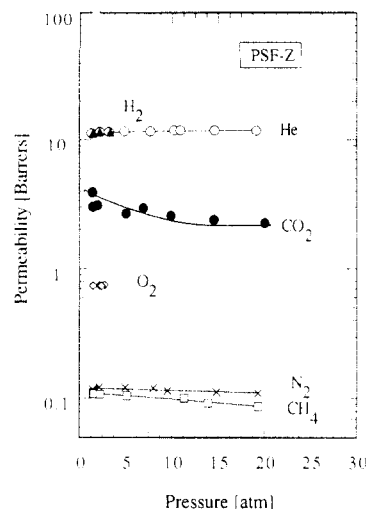


**Figure 14.** Relationship between the  $O_2$  permeability coefficient and the sub- $T_g$  relaxation temperature  $T_{\gamma 2}$ . Open dots represent polysulfones reported here, while solid points are for polysulfones described elsewhere.<sup>8-12</sup>

apparent relationship between permeability and  $T_{\gamma 2}$ , no relationship at all was found between gas permeability and  $T_{\gamma 1}$  or  $T_g$  for these polysulfones.

#### Effect of Symmetric and Unsymmetric Methyl Group Placement

A previous study showed that the symmetry of methyl group substitutions on the bisphenol monomer of polysulfones also has a significant effect on gas transport as well as density and  $T_g$ . The symmetric polymer, tetramethyl-Bisphenol A polysulfone (TMPSF), has a very open and rigid structure and gas permeability coefficients that are approximately 3 times greater than those for PSF. In contrast, the unsymmetric dimethyl-Bisphenol A polysulfone (DMPSF) has a lower free volume, lower  $T_g$ , and lower permeability coefficients than Bisphenol A polysulfone. Replacement of the isopropylidene unit of DMPSF with a cyclohexyl group (DMPSF-Z) also resulted in an even more packed structure. In this study, the polysul-



**Figure 15.** Pressure dependence of  $He$ ,  $H_2$ ,  $O_2$ ,  $N_2$ ,  $CH_4$ , and  $CO_2$  permeability coefficients for PSF-Z at 35 °C.

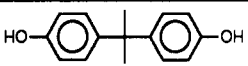
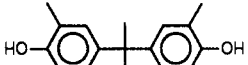
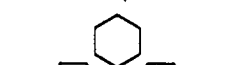

fone for which the phenyl rings are connected by a single carbon of a cyclohexyl group (PSF-Z) has been synthesized and evaluated. The structures of these polysulfones are shown in Table VIII. The objective of this analysis is to draw a parallel between the effect of unsymmetric dimethyl substitution on properties and those of unsymmetric ring connections discussed above.

The permeability coefficients for PSF-Z, shown in Figure 15, remain constant or decrease with pressure for all gases; no plasticization was observed at these pressures. In addition, minimal conditioning effects were noted. In Table VIII, permeability coefficients for PSF-Z are compared with those for PSF, DMPSF, and DMPSF-Z from McHattie et al.<sup>8</sup> For all gases, the permeability coefficients are lower for PSF-Z than for PSF and, following the typical trade-off with permeability, the selectivities are higher. As listed in Table IX, this decrease in permeability is accompanied by a decrease in fractional free volume. Although the cyclohexyl group is bulky and imparts some rigidity to the polymer chain as indicated by the higher  $T_g$ , it does not hinder chain packing. It is likely that the cyclohexyl group takes on conformations that allow it to fill the unoccupied space between chains and, thus, reduce free volume.

Dimethyl substitution onto the Bisphenol Z monomer results in a further decrease in permeability. The selectivities for  $O_2/N_2$  and  $CO_2/CH_4$  in DMPSF-Z are the highest reported for the polysulfone family. Similar to the unsymmetrical isomer cases, the dimethyl substitution results in a lower  $T_g$  and FFV. As shown in Figure 7, the permeability coefficients for this group of polymers correlate well with inverse fractional free volume.

As discussed previously,<sup>42</sup> PSF-Z and PSF have similar sub- $T_g$  spectra; however, the sub- $T_g$  relaxation temperature  $T_{\gamma 2}$  is higher for PSF-Z. The temperature at which this relaxation occurs has been associated with the degree of intermolecular packing in the polymer matrix (Figure 13). DMPSF and DMPSF-Z both have two sub- $T_g$  relaxations, listed in Table IX, which, as discussed earlier,<sup>42</sup> can be associated with the respective motions of the bisphenol and sulfone monomer groups. The sub- $T_g$  relaxation temperature  $T_{\gamma 1}$  indicates that the motions involving the dimethyl-Bisphenol A monomer unit are more restricted than those involving Bisphenol A. However, the  $\gamma_1$  peaks for DMPSF-Z and DMPSF are both much broader than that for TMPSF (Figure 16). In fact, the shapes of the  $\gamma_1$  peaks for the dimethyl polysulfones are similar to the broad  $\gamma_1$  peaks of the polysulfones with meta linkages.

**Table VIII**  
**Permeability and Selectivity Coefficients for Polysulfones with Unsymmetric Methyl Substitutions at 35 °C**

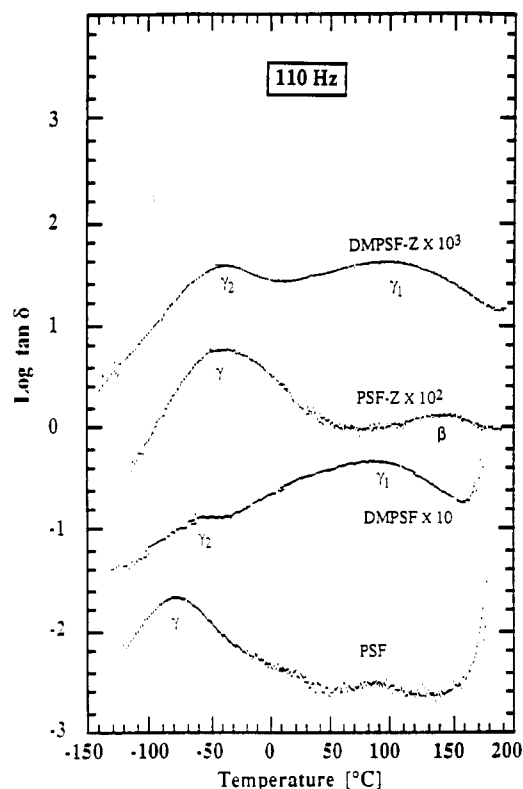
polymer	bisphenol monomer	$P_{CO_2}$ , <sup>a</sup> barrer <sup>b</sup>	$\alpha^*_{CO_2/CH_4}$ <sup>a</sup>	$P_{O_2}$ , <sup>c</sup> barrer <sup>b</sup>	$\alpha^*_{O_2/N_2}$ <sup>c</sup>	$P_{He}$ , <sup>a</sup> barrer <sup>b</sup>	$\alpha^*_{He/CH_4}$ <sup>a</sup>	$\alpha^*_{He/H_2}$ <sup>c</sup>
PSF		5.6	22	1.4	5.6	13	49	0.93
DMPSF		2.1	30	0.64	7.0	12	170	1.1
PSF-Z		2.54	25	0.74	6.5	11.7	117	1.0
DMPSF-Z		1.4	34	0.41	7.2	11	280	1.2

<sup>a</sup> Data at 10 atm. <sup>b</sup> Barrer =  $10^{-10}[\text{cm cm}^3(\text{STP})]/(\text{cm}^2 \text{ s cmHg})$ . <sup>c</sup> Data at 1 atm.

**Table IX**  
**Properties of Polysulfones with Unsymmetric Methyl Substitutions**

polymer	$T_g$ , °C	$T_\beta$ , °C	$T_{\gamma_1}$ , °C	$T_{\gamma_2}$ , °C	$\rho$ , g/cm <sup>3</sup>	FFV, $(V - V_0)/V$	$d$ spacing, Å	$[\eta]$ , <sup>a</sup> dL/g
PSF	186	85		-80	1.240	0.156	4.9	0.4
DMPSF	180		80	-60	1.213	0.149	5.0	1.0
PSF-Z	211	140		-35	1.237	0.146	4.9	1.3
DMPSF-Z	197		100	-35	1.227	0.136	5.0	1.1

<sup>a</sup> In chloroform at 25 °C.



**Figure 16.** Tan  $\delta$  at 110 Hz as a function of temperature showing the sub- $T_g$   $\gamma$  peaks for dimethyl-substituted polysulfones. Assignments are described in the text.

Perhaps the large  $\gamma_1$  peaks for DMPSF and DMPSF-Z are due to not only a restriction of phenylene motions caused by the methyl addition but also the unsymmetric nature of the substitution which leads to an increase in peak amplitude.

### Discussion

The effect of dimethyl substitutions onto the phenylene rings of polysulfones is very similar to the effect of meta bond connection of these rings. In both cases, the un-

symmetric polysulfones consistently have lower permeabilities, lower glass transition temperatures, and higher selectivities than their symmetric counterparts. This effect appears to arise from both intermolecular and intramolecular factors. The unsymmetric polysulfone chains are more well packed in the glassy and melt states than their symmetric counterparts; thus, they have lower FFV and permeability. This agrees with numerous other papers in the literature that compares isomers within several different polymer families. While the meta isomer is typically more dense than its para counterpart for aromatic polymers, Stern et al.<sup>2</sup> report that the two unsymmetric polyimides, PMDA-3,3'-BDAF and 6FDA-3,3'-ODA, have lower densities than their symmetric isomers, PMDA-4,4'-BDAF and 6FDA-4,4'-ODA. Their  $d$  spacings from X-ray diffraction, however, show that the mean interchain spacing is much lower for the meta-linked polyimide than for its para isomer and suggest that the former is actually more packed. The unsymmetric polymers consistently have lower permeabilities and glass transition temperatures than their symmetric isomers as do the polysulfone isomers.

The lower  $T_g$  for the meta isomers of polysulfone may contribute some to their higher density and lower fractional free volume as previously suggested for stereoisomers;<sup>7</sup> however, this argument does not completely explain the isomeric phenomenon at issue here as described above. In addition to the differences in the specific volume, it appears that there are other fundamental differences in the glassy state of these isomers. The unsymmetric polymers have lower thermal expansion coefficients below  $T_g$  which Numata et al.<sup>43</sup> associated with the linearity of the molecular structure for several polyimides.

The lower gas solubility coefficients for the meta-linked polysulfones stem generally from their lower fractional free volume as the results in Figure 7 indicate. In terms of the dual mode model, the unsymmetric polymers consistently have lower Langmuir capacity terms than their symmetrical counterparts. This can be related to their lower amount of unrelaxed volume in the glassy state stemming from both a lower  $T_g$  and a smaller difference

in thermal expansion coefficients between the rubbery and glassy states. Further analysis of the polysulfone sorption data is given elsewhere.<sup>39</sup>

As the sub- $T_g$  spectra in Figures 10 and 11 show, bond location or symmetry affects the intramolecular mobility of these polysulfones. The  $T_{\gamma_1}$  for PSF-M is 115 °C higher than  $T_{\gamma_2}$ , perhaps reflecting the hindered mobility about the asymmetric meta linkage compared to that about the para linkage. Such restrictions in local mode motions for the unsymmetric monomer unit are not the only reason for lower penetrant mobility in these materials since we have shown that other polysulfones have their sub- $T_g$  relaxations at even higher temperatures yet their gas permeabilities are higher not lower, e.g., hexamethylbiphenol polysulfone.<sup>10</sup> We noted that because of their unsymmetric bond locations, the meta-linked phenyl rings must involve more of the polymer chain to rotate than the para-linked polymer, and, thus, because of this intramolecular mobility constraint and the more packed environment of the unsymmetric matrix,  $T_{\gamma_1}$  is higher. In contrast, the  $T_g$  for the unsymmetric polymer is consistently lower than that for its symmetric counterpart. The difference between  $T_g$  and  $T_{\gamma_1}$  is much less for the meta isomers than for the para isomers. Perhaps because the meta linkage requires more of the polymer chain to be involved in the sub- $T_g$  motion, the glass transition may follow with a relatively small further addition of thermal energy and, thus, the  $T_g$  is lower for the unsymmetric aromatic polymers than for the symmetric ones.

## Summary

The lower permeability and higher selectivity for the polysulfones with meta linkages appears to stem from both mobility constraints imposed by molecular geometry and more efficient intermolecular packing. The unsymmetrical polysulfones have lower glass transition temperatures, lower free volumes, but higher sub- $T_g$  relaxation temperatures. Whether the unsymmetric nature is a result of meta bond linkages or dimethyl substitutions, the effect is the same. This suggests that when an unsymmetric component is added to the polymer chain, the polymer may take on conformations that increase polymer packing. This increased packing, however, is not limited to polymers. A survey of simple liquid isomers has shown that this is a general trend for unsymmetric aromatic compounds. If the barriers to rotation are higher for an unsymmetric molecule, as suggested by the sub- $T_g$  data and Monte Carlo simulation,<sup>16</sup> and its occupied volume is higher than for its symmetric counterpart, the result could be a higher activation energy for diffusive jumps combined with lower fractional free volume. Both of these factors appear to contribute to the lower permeability and higher selectivity coefficients for the unsymmetric aromatic polymers. The lower  $T_g$  of the meta isomer, which is partly responsible for the higher density of these materials as previously discussed, may also be related to the extent of segmental motion involved in the sub- $T_g$  relaxation. There is an interesting contrast in the effects that symmetry has on properties of polymers with aromatic backbones compared to those with carbon-carbon backbones, viz., vinyl vs vinylidene series. Perhaps molecule modeling will be able to provide insight about this difference in the near future.

**Acknowledgment.** This research was supported by the Department of Energy, Basic Sciences Program, through Grant DE-FG05-86ER13507 and the Separations Research Program at The University of Texas at Austin. C.L.A. acknowledges the Shell Oil Co. Foundation and

the Plastics Institute of America for fellowship support.

## References and Notes

- (1) Coleman, M. R.; Koros, W. J. *J. Membr. Sci.* **1990**, *50*, 285.
- (2) Stern, S. A.; Mi, Y.; Yamamoto, H. *J. Polym. Sci., Polym. Phys. Ed.* **1989**, *27*, 1887.
- (3) Sykes, G. F.; St. Clair, A. K. *J. Polym. Sci.* **1986**, *32*, 3725.
- (4) Tanaka, K.; Kita, H.; Okamoto, K.; Nakamura, A.; Kusuki, Y. *Polym. J.* **1990**, *22*, 381.
- (5) Light, R. R.; Seymour, R. W. *Polym. Eng. Sci.* **1982**, *22*, 229.
- (6) Sheu, F. R.; Chern, R. T. *J. Polym. Sci., Polym. Phys. Ed.* **1989**, *27*, 1121.
- (7) Min, K. E.; Paul, D. R. *J. Polym. Sci., Polym. Phys. Ed.* **1988**, *26*, 1021.
- (8) McHattie, J. S.; Koros, W. J.; Paul, D. R. *Polymer* **1991**, *32*, 840.
- (9) Muruganandam, N.; Paul, D. R. *J. Membr. Sci.* **1987**, *34*, 185.
- (10) Aitken, C. L.; Koros, W. J.; Paul, D. R. *Macromolecules* **1992**, in press.
- (11) McHattie, J. S.; Koros, W. J.; Paul, D. R. *Polymer* **1991**, *32*, 2618.
- (12) McHattie, J. S.; Koros, W. J.; Paul, D. R. *Polymer* **1992**, in press.
- (13) McHattie, J. S.; Koros, W. J.; Paul, D. R. *J. Polym. Sci., Polym. Phys. Ed.* **1991**, *29*, 731.
- (14) Hellums, M. W.; Koros, W. J.; Husk, G. R.; Paul, D. R. *J. Membr. Sci.* **1989**, *46*, 93.
- (15) Barbari, T. A.; Koros, W. J.; Paul, D. R. *J. Membr. Sci.* **1989**, *42*, 69.
- (16) Pavlova, S. S. A.; Timofeeva, G. I.; Ronova, J. A. *J. Polym. Sci., Polym. Phys. Ed.* **1980**, *18*, 1175.
- (17) Sundararajan, P. R. *Macromolecules* **1990**, *23*, 2600.
- (18) Tonelli, A. E. *Macromolecules* **1973**, *6*, 503.
- (19) Hopfinger, A. J.; Pearlstein, R. A. *J. Macromol. Sci., Phys.* **1987**, *B26*, 359.
- (20) Hopfinger, A. J.; Koehler, M. G.; Pearlstein, R. A. *J. Polym. Sci., Polym. Phys. Ed.* **1988**, *26*, 2029.
- (21) Mohr, J. M.; Paul, D. R. *J. Appl. Polym. Sci.* **1991**, *42*, 1711.
- (22) Boyer, R. F. *J. Appl. Phys.* **1954**, *25*, 825.
- (23) Beaman, R. G. *J. Polym. Sci.* **1952**, *9*, 470.
- (24) Gibbs, J.; Di Marzio, E. *J. Chem. Phys.* **1958**, *28*, 373, 807.
- (25) Mohanty, D. K.; Sachdeva, Y.; Hedrick, J. L.; Wolfe, J. F.; McGrath, J. E. *Polym. Prepr. (Am. Chem. Soc., Div. Polym. Chem.)* **1984**, *25*, 19.
- (26) Mohanty, D. K. Ph.D. Dissertation, Virginia Polytechnic Institute and State University, 1983.
- (27) McHattie, J. S. Ph.D. Dissertation, University of Texas at Austin, 1990.
- (28) Van Krevelen, D. W.; Hoftyzer, P. J. *Properties of Polymers*; Elsevier: New York, 1976.
- (29) Bondi, A. *Physical Properties of Molecular Crystals, Liquids, and Glasses*; Wiley: New York, 1968.
- (30) Zoller, P. *J. Polym. Sci., Polym. Phys. Ed.* **1982**, *20*, 1453.
- (31) Zoller, P. *J. Polym. Sci., Polym. Phys. Ed.* **1978**, *16*, 1261.
- (32) Koros, W. J.; Paul, D. R.; Rocha, A. A. *J. Polym. Sci., Polym. Phys. Ed.* **1976**, *14*, 687.
- (33) Koros, W. J.; Paul, D. R. *J. Polym. Sci., Polym. Phys. Ed.* **1978**, *16*, 1947.
- (34) Paul, D. R. *J. Polym. Sci.: Part A-2* **1969**, *7*, 1811.
- (35) Petropoulos, J. H. *J. Polym. Sci.: Part A-2* **1970**, *8*, 1797.
- (36) Toi, K.; Morel, G.; Paul, D. R. *J. Appl. Polym. Sci.* **1982**, *27*, 2997.
- (37) Muruganandam, N.; Koros, W. J.; Paul, D. R. *J. Polym. Sci., Polym. Phys. Ed.* **1987**, *25*, 1999.
- (38) Maeda, Y.; Paul, D. R. *J. Polym. Sci., Polym. Phys. Ed.* **1987**, *25*, 1005.
- (39) Aitken, C. L. Ph.D. Dissertation, University of Texas at Austin, 1992.
- (40) Lange, N. A. *Lange's Handbook of Chemistry*, 12th ed.; Den, J. A., Ed.; McGraw-Hill: New York, 1979.
- (41) Lide, D. R. *CRC Handbook of Chemistry and Physics*, 71st ed.; CRC Press: Boca Raton, FL, 1990.
- (42) Aitken, C. L.; McHattie, J. S.; Paul, D. R. *Macromolecules* **1992**, in press.
- (43) Numata, S.; Kinjo, N. *Polym. Eng. Sci.* **1988**, *28*, 906.